AMERICAN SCIENTIFIC PUBLISHERS

Journal of Advanced Physics
Vol. 5, pp. 1–5, 2016
(www.aspbs.com/jap)

ARTICLE

Core-Polarization Effects on the Isoscalar and Isovector Transitions in ^{24}Mg Using Extended Shell Model

Khalid S. Jassim* and Rawaa A. Abdul-Nabi

Department of Physics, College of Education for Pure Sciences, University of Babylon, P.O. Box 4, Hilla-Babylon, Iraq

Electron scattering form factors as well as reduced transition probabilities for the isoscalar and isovector states of the ^{24}Mg nucleus in sdpf shells have been studied by considering the higher energy configurations outside the sd-shell, which are called core-polarization (CP) effects. The core polarization effects are calculated with the Michigan three-range Yakawa as a realistic interaction. The wave functions of radial single particle matrix elements have been calculated with harmonic oscillator potential. The predicted form factors are compared with the available experimental data. Very good agreements are obtained for all nuclei under study. Results from electron scattering form factors and reduced transition probabilities show that the large scale model space with core polarization effects (inclusion of the higher energy configurations with $6\hbar\omega$ excitation) enhanced the results to become closed to the experimental data.

KEYWORDS: Sd-Shell Nuclei, Longitudinal form Factors, Transverse form Factors, NuShell, Nuclear Structure.

1. INTRODUCTION

The first idea about the discovery of the theoretical scattering by Mott in 1929.[1] He was able to find a scattering point without dimensions, while the experimental detection of scattering of electron from nuclei to a separated level by Collins and Waldman 1940.[2] The electron scattering is the best method to clarify the distribution of charge in nucleus, in addition to the fact that the electron particle point consequently the electron can readily accelerated.[3]

Electron scattering form factor is the factor determining the shape of the spherical nucleus. It depends on current, magnetization distribution and the charge in the target nucleus, which regarded as a function of the momentum transfer (q) and it could be found experimentally through knowing the scattering angle and the energies of the incident and scattered electrons.[4] The form factor is divided into two kinds, longitudinal (Coulomb) form factor, which represents by Fourier transform of the charge density[5] and provide all information about the nuclear charge distribution. The other kind of form factor is transverse form factor, which is the Fourier transform of the current density this kind contain the information about the magnetization distributions and nuclear current.[5] According to the parity selection rules the transverse form factor can be sorted into transverse electric and magnetic electron scattering form factor.[6]

The two body matrix element (TBME) for effective interaction between nucleon–nucleon $\langle x_1 x_2|H|x_3 x_4\rangle_{TJ}$ it represents a formula connect angular momentum functions, where H represent the effective interaction, $(x_1, x_2, x_\downarrow(3), x_\downarrow 4)$ are represent single-particle orbits and T and J are represent the spin and isospin of the coupled nucleons.

The Michigan three-range Yukawa interaction (M3Y)[7] will be used in various models and its give matrix elements similar to some dependable shell-model interactions, the M3Y-type interactions has been obtained from the realistic NN interaction by fitting the Yukawa functions to the G-matrix given by the sum of the Yukawa functions.[8] M3Y-type interactions have successfully been used for nuclear reactions,[9] involved electron scattering. A kind of the M3Y-type interactions can be used to the electron scattering form factor calculations.

Recently many paper by Jassim and et al.[10–14] have been performed many studies about nuclear structure of some light nuclei in p, sd and fp model space using shell model calculations. These studies give good agreement in energy levels and electron scattering form factors calculations comparing with the experimental data. Majeed et al.[15] have been studied the Longitudinal and transverse electron scattering form factors for some positive and negative parity states of stable odd-A nuclei: ^{7}Li, ^{13}C and ^{17}O by considering the higher energy configurations outside the

*Author to whom correspondence should be addressed.
Email: Khalid_ik74@yahoo.com
Received: 4 August 2015
Accepted: 17 August 2015

p- and *sd*-shells. The ground-state spins and parities of the odd-A phosphorus isotopes[25–47] P were studied with the relativistic mean-field (RMF) model and relativistic elastic magnetic electron-scattering theory (REMES) by Ref. [16].

The purpose of the present work is to account the longitudinal electron scattering form factors with the effect of the CP in some *sdfp*-shell. Two shell model codes, CPM3Y and NuShell for windows have been use in our calculations. The large scale two-body *sdpf* now effective interaction is used with M3Y as a residual interaction for the CP calculation for *sdpf*-shell was used in this research. The Hamiltonians *sdpf* interaction has been used to give the $1d_{5/2}$, $1d_{3/2}$, $2s_{1/2}$, $1f_{7/2}$, $1f_{5/2}$, $2p_{3/2}$, and $2p_{1/2}$ shell model wave function, which is used for ^{24}Mg in this study. The wave function of radial single matrix elements have use Harmonic Oscillator (HO).

2. THEORY

The many particle matrix elements composed of two branch one is for the Core-polarization (CP) matrix elements, and the other is for the Model space (MS) matrix elements:[17]

$$\langle \sqcap_f \| \hat{O}^{\eta}_{\wedge} \| \Pi_i \rangle = \langle \Pi_f \| \hat{O}^{\eta}_{\wedge} \| \Pi_i \rangle_{MS} + \langle \Pi_f | \square | \delta \hat{O}^{\eta}_{\wedge} | \square | \Pi_i \rangle_{CP} \tag{1}$$

When the states $|\sqcap_i\rangle$ and $|\sqcap_f\rangle$ are Clarifies by the model-space wave functions. Greek symbols are used to refer to quantum numbers in coordinate space and isospin, i.e., $\sqcap_f = J_f T_f$, $\Pi_i = J_i T_i$ and $\wedge = JT$.

The equations of model space matrix elements can be written as:

$$\langle \sqcap_f \| \hat{O}^{\eta}_{\wedge} \| \sqcap_i \rangle_{MS} = \sum_{\alpha,\beta} A^{X}_{X_i X_f}(\alpha,\beta) \langle \alpha \| \hat{O}^{\eta}_{\wedge} \| \beta \rangle \tag{2}$$

Similarly, the core-polarization matrix elements are given by:

$$\langle \sqcap_f \| (\square | \delta \hat{O}^{\eta}_{\wedge} |) | \square | \Pi_i \rangle_{cp} = \sum_{\alpha,\beta} A^{X}_{X_i X_f}(\alpha,\beta) \langle \alpha \| \hat{O}^{\eta}_{\wedge} \| \beta \rangle \tag{3}$$

where $A^{X}_{X_i X_f}(\alpha,\beta)$ is the single-particle matrix elements and α, β indicate the initial and final single particle states.

The first order perturbation theory says that, the single-particle matrix element for the higher-energy configurations can be expressed as:[18]

$$\langle \alpha | \delta \hat{O}^{\eta}_{\wedge} | \beta \rangle = \left\langle \alpha \left| V_{12} \frac{P}{E_f - H(0)} \hat{O}^{\eta}_{J} \right| \beta \right\rangle + \left\langle \alpha \left| \hat{O}^{\eta}_{J} \frac{P}{E_i - H(0)} V_{12} \right| \beta \right\rangle \tag{4}$$

The operator Q is the projection operator onto the space outside the model space. For the residual interaction, $V_{\rm res}$, we adopt the M3Y, $H(0)$ is the unperturbed Hamiltonian, E_i and E_f represents the true energy initial and final states of the system Eq. (4) is written as.[18]

$$\begin{aligned} \langle \alpha | \delta \hat{O}^{\eta}_{J} | \beta \rangle = \sum_{\alpha_1,\alpha_2,X} & \frac{(-1)^{\beta+\alpha_2+X}}{e_\beta - e_\alpha - e_{\alpha_1} - e_{\alpha_2}} (2X+1) \\ & \times \begin{Bmatrix} \alpha & \beta & \wedge \\ \alpha_1 & \beta_1 & X \end{Bmatrix} \times \langle \alpha\alpha_1 | V_{12} | \beta\alpha_2 \rangle_{\Gamma} \\ & \times \langle \alpha_1 \| \hat{O}^{\eta}_{\wedge} \| \alpha_2 \rangle \\ & \times \sqrt{(1+\delta_{\alpha_1\alpha})(1+\delta_{\alpha_2\beta})} + A \end{aligned} \tag{5}$$

where e is the single-particle energy, The indices $\alpha_1 \equiv j_p t_p$ and $\alpha_2 \equiv j_h t_h$ runs over particle and hole states, respectively, $\hat{T}^{\eta}_{\Lambda}$ represents single-particle transition operator of rank $I_\Lambda = 0$ or 1 are means isoscalar or isovector contribution and of rank L in space coordinate. The CP parts taken up to $4\hbar\omega$ allow particle-hole excitations from the core and model space into higher orbits. The equation of reduced single particle matrix-element given by:

$$\langle \alpha \| \hat{O}^{\eta}_{LT} \| \beta \rangle = \sqrt{\frac{2T+1}{2}} \sum_{t_Z} P_T(t_Z) \langle n_\alpha l_\alpha j_\alpha || \hat{O}^{\eta}_{LT} | n_\beta l_\beta j_\beta \rangle \tag{6}$$

where:

$$P_T(t_z) = \begin{cases} 1 & \text{for } T = 0 \\ (-1)^{1/2 - t_z} & \text{for } T = 1 \end{cases} \tag{7}$$

$t_{Z=1/2}$ for proton and $t_{Z=-1/2}$ for neutron.

Electron scattering form factor involving angular momentum J and momentum transfer q, between the initial and final nuclear shell model states of spin $J_{i,f}$ and isospin $T_{i,f}$ are[19]

$$\begin{aligned} |F^{\eta}_{L}(q)|^2 = \frac{4\pi}{Z^2(2J_i+1)} \Bigg| \sum_{T=0,1} & (-1)^{T_f - T_{Z_f}} \\ & \times \begin{pmatrix} T_f & T & T_i \\ -T_{Z_f} & M_T & T_{Z_i} \end{pmatrix} \times \langle \sqcap_f \| \hat{O}^{\eta}_{LT}(q) \| \sqcap_i \rangle |^2 \\ & \times |F_{c\cdot m}(q)|^2 \times |F_{f\cdot s}(q)|^2 \end{aligned}$$

where $F_{\rm cm}(q) = e^{q^2 b^2/4A}$ is the correction for the lack of translation invariance in the shell model. A and b are the mass number and the harmonic oscillator size parameter, respectively.

The single-particle energies are calculated according to:[18]

$$e_{nlj} = \left(2n + l - \frac{1}{2}\right)\hbar\omega + \begin{cases} -\frac{1}{2}(l+1)\langle f(r)\rangle_{nl} & \text{for } j = l - \frac{1}{2} \\ \frac{1}{2}(l)\langle f(r)\rangle_{nl} & \text{for } j = l + \frac{1}{2} \end{cases}$$

With:

$$\langle f(r)\rangle_{nl} \approx 20A^{-2/3}\ \text{Mev}$$
$$\hbar\omega = 45A^{-1/3} - 25A^{-2/3} \tag{8}$$

When collecting of the spin-orbit potential part ν_{12}^{LC}, long-range tensor part ν_{12}^{TN}, and central potential part ν_{12}^{C} consists the realistic M3Y effective NN interaction, which is used in the electron scattering ν_{12}:[20]

$$\nu_{12} = \nu_{12}^{(C)} + \nu_{12}^{(LS)} + \nu_{12}^{(TN)} \tag{9}$$

The two-body matrix elements of the realistic M3Y effective NN interaction divide in to branches are the central potential, spin-orbit potential, and tensor potential, respectively.

$$\langle j_1 j_2|V_{\text{res}}|j_3 j_4\rangle_{\sqcap} = \langle j_1 j_2|V_C|j_3 j_4\rangle_{\sqcap} + \langle j_1 j_2|V_{s\cdot l}|j_3 j_4\rangle_{\sqcap} + \langle j_1 j_2|V_{\text{ten}}|j_3 j_4\rangle_{\sqcap} \tag{10}$$

The reduced transition probability is related to the form factor at the photon point, which is given by.[21]

$$B(CJ) = \frac{|(2J+1)!!|^2}{4\pi}\frac{Z^2e^2}{k^{2L}}|F_J^{C_0}(q=k)|^2 \tag{11}$$

where $q = k = E_x/\hbar C$ is the momentum transfer and the term $|F \downarrow J \uparrow (C \downarrow 0)(q = k| \uparrow 2)$ is the longitudinal (Coulomb) form factor at $k = q$.

$$|F_J^{C_0}(k)|^2 = \frac{4\pi}{(2J_i+1)Z^2}\left|\int_0^\infty dr r^2 j_J(kr)\rho_J(i,f,r)\right|^2 \tag{12}$$

Here $\rho_J(i,f,r)$ is the transition charge density for the initial and final states.

For the two-body matrix elements of the residual interaction $\langle\alpha\alpha 2|V12|\beta\alpha 1\rangle$, which appear in Eqs. (5) and (11), the M3Y interaction of Bertch et al.[7] is adopted. The interaction is taken between a nucleon in any core orbit and a nucleon that is excited to higher orbits with the same parity and with the required multipolarity (Λ) and between a nucleon in any *sd* orbits and that is excited to higher orbits with the same parity and with the required multipolarity. This interaction is given in the *LS* coupling.

3. RESULTS AND DISCUSSION

The shell model calculations in the present paper are performed using a computer program, CPM3Y to calculate form factors with CP effects. The OBDM elements are calculated by using the shell model NUSHELL code with *sdpfnow* as effective interactions in large-scale *psd* with the ^{16}O as the inert core. The radial wave function for the single-particle matrix elements have been calculated with the HO potential with size parameter $(b) = 1.813$[22] fm.

Table I shows a Comparison of the probability density values obtained from the shell model calculations with the experimental values for isoscalar and isovector state in the ^{24}Mg nucleus. It can be seen that the theoretical probabilities density values reproduce the data quite well.

Table I. Theoretical calculation of the probabilities density (in units of e^2 fm^4) for isoscalar and isovector state in the ^{24}Mg nucleus in comparison with experimental values and other work.

Transition	Exp.	Present work
B(C2) $(0^+\ 0) \rightarrow (2_1^+\ 0)$	428.9 ± 8.74[23, 24]	524.7
B(C2) $(0^+\ 0) \rightarrow (2_2^+\ 0)$	22.37 ± 0.053[23, 24]	17.85
B(C4) $(0^+\ 0) \rightarrow (4_2^+\ 0)$	43 ± 6[25]	–
B(M1) $(0^+\ 0) \rightarrow (1_1^+\ 1)$	0.886 ± 0.16[26]	1.129
B(M1) $(0^+\ 0) \rightarrow (1_2^+\ 1)$	2.705 ± 0.36[26]	3.318
B(M1) $(0^+\ 0) \rightarrow (1_3^+\ 1)$	–	1.986

3.1. The Isoscalar State

The isoscalar longitudinal C2 form factors for 2_1^+ (1.37 MeV) state in the ^{24}Mg nucleus are illustrated in Figure 1. These calculations were implemented by program in our computer with restricting $1f_{7/2}$, $2f_{5/2}$ orbits that means the eight nucleons (4 protons and 4 neutrons) distributed over an extended model space orbits ($2p_{3/2}$, $2p_{1/2}$, $2s_{1/2}$, $1d_{5/2}$, $1d_{3/2}$). The solid and dashed curves represent the calculation extended model space (*sdp* shell) with and without CP effects, respectively, where the calculations with CP effects are calculated by using microscopic theory with CPM3Y code. The results of C2 form factors with the CP effect give a good applicability comparison with experimental data from Ref. [25] for all momentum transfer region between (0.0 and 2.5) fm^{-1}, while the results without CP effects give a poor applicability comparing with the experimental data. This signifies that using extended model space with CP effects enhanced the C2 results comparing with calculations without CP effects.

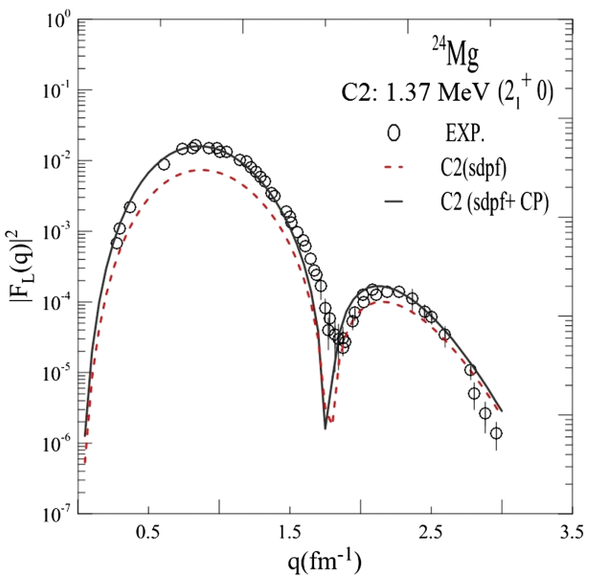

Fig. 1. Inelastic longitudinal (C2) form factors for the 2^+ (1.37 MeV) state in the ^{24}Mg using the *sdpfnow* effective interaction, with (solid curves) and without (dashed curves) CP effects. The experimental data are taken from [25], G. C. Li, et al., *Phys. Rev. C* 9, 1861 (**1974**). © 1974.

Figure 2 shows the isoscalar C2 form factor for transitions from the ground state (0^+ 0) to the excited state (2_2^+ 0) by the electron, where the transition energy to this state at 4.24 MeV. The extended model space calculations (dashed curves) failed to describe the experimental data form Ref. [27] in all momentum transfers region, while the form factor calculations with CP effects (solid curves) improvement measured form factors in the first maximum diffraction especially from the momentum transfer region between (0.0–1.3) fm^{-1}. The result start to far from the experimental data up to $q = 3.0$ fm^{-1}.

Figure 3 shows the Coulomb form factors (C4) using the ground state charge density distribution in even–even $N = Z$ *sd*-shell nucleus ^{24}Mg for transition from (0^+ 0) to state (4_2^+ 0) with excitation energy 6.00 MeV. The adding CP effects with extended model space (solid curves) described the experimental data[28] in the momentum transfer region between (0.5–2.1) fm^{-1}. But, the *spd* results only without CP effects fail to describe the experimental data in the same momentum transfer region.

3.2. The Isovector State

The results of the magnetic form factors (M1) for 1_1^+ (9.967 MeV) in ^{24}Mg are illustrated in Figure 4. We noticed that the M1 results with and without CP effect described the available experimental data from Ref. [22] in the first maximum diffraction at the momentum transfer region between (0.0–1.5) fm^{-1}, in the other side, we note that the results with using CP effects as a solid curves shifted the second and third peak (maximum diffraction) to the right, where the position of the three maximum diffraction for the scattered electron with CP effect included at 0.5, 1.6 and 2.3 fm^{-1}, respectively, while without inclusion CP effect, the three maximum diffraction are 0.45, 1.5 and 2.2 fm^{-1} for the first, second and third maximum diffraction, respectively.

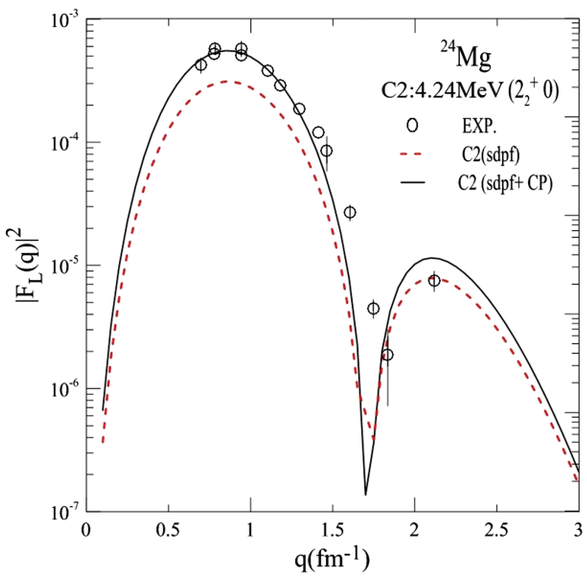

Fig. 2. Inelastic longitudinal (C2) form factors for the 2_2^+ (4.24 MeV) state in the ^{24}Mg using the *sdpfnow* effective interaction, with (solid curves) and without (dashed curves) CP effects. The experimental data are taken from [27], H. Zarek, et al., *Phys. Lett.* 80B, 2 (**1978**). © 1978.

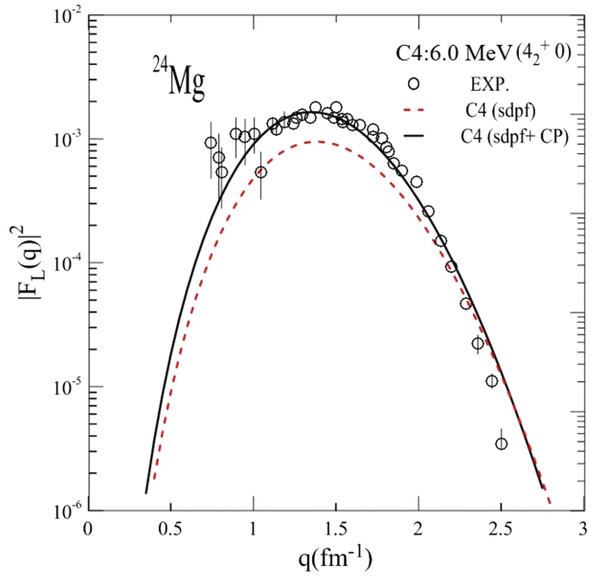

Fig. 3. Inelastic longitudinal (C4) form factors for the 4_2^+ (6.00 MeV) state in the ^{24}Mg nucleus using the *sdpf now* effective interaction, with (solid curves) and without (dashed curves) CP effects. The experimental data are taken from [28], Y. Horikawa, et al., *Phys. Lett.* 39B, 9 (**1971**). © 1971.

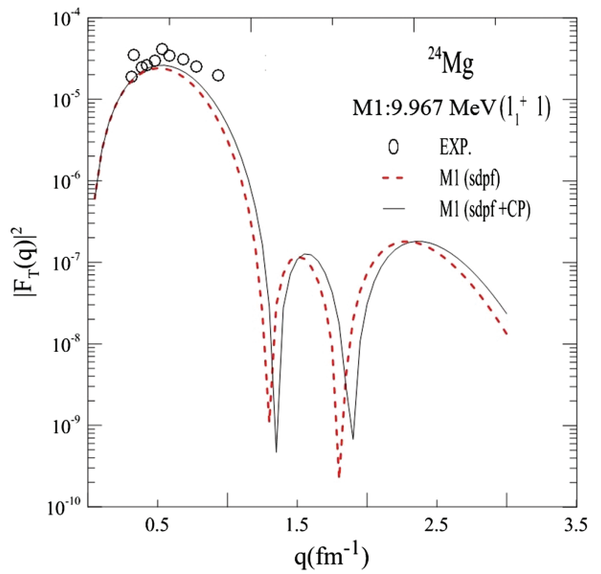

Fig. 4. Inelastic transverse (M1) form factors for the 1_1^+ (9.967 MeV) state in the ^{24}Mg nucleus using the *sdpfnow* effective interaction, with (solid curves) and without (dashed curves) CP effects. The available data, shown as circles from [22], B. A. Brown, et al., *Phys. Rev.* 101, 313 (**1983**). © 1983.

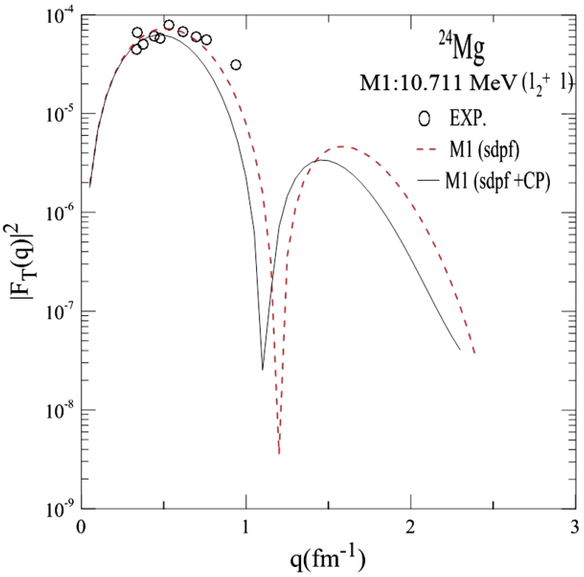

Fig. 5. Inelastic transverse (M1) form factors for the 1_2^+ (10.711 MeV) state in the ^{24}Mg nucleus using the *sdpf now* effective interaction, with (solid curves) and without (dashed curves) CP effects. The available data, shown as circles from [22], B. A. Brown, et al., *Phys. Rev.* 101, 313 (**1983**). © 1983.

Figure 5 shows the isovector magnetic form factors with *spdf* shell model for transitions from the ground state 0^+ 0 to the excited state 1_2^+ 1 with excitation energy 10.711 MeV in the ^{24}Mg. The results of M1 form factors with and without inclusion CP effects by using microscopic theory give a good agreement comparing with the available experimental data[22] in first maximum region ($0.0 < q < 0.5$) fm^{-1}. The first and second maximum diffraction without inclusion CP effects are 0.6 and 1.6 fm^{-1}, respectively. While the first and second maximum region with inclusion CP effects are 0.5 and 1.5 fm^{-1}, respectively. From these results, we concluded that the CP effects shifted the first and second peak toward decreases momentum transfer by 0.1 fm^{-1}.

4. CONCLUSION

Electron scattering form factors and reduced transition probabilities for the isoscalar and isovector states of the ^{24}Mg nucleus in large scale shell model have been studied by considering the higher energy configurations outside the *sdpf* shells. The *sdpfnow* interactions for *sdfp* shells are used with the M3Y as a residual interaction for the CP effect calculations. The effect of CP is found essential in both the transition strengths and momentum transfer dependence, and gives a good description of the data using large scale shell model with adjustable any parameters. The use of large scale shell model with a modern interaction may give a better description of the form factors.

References and Notes

1. N. F. Mott, *Proc. Roy. Soci. Ser. A* 124, 425 (**1929**).
2. B. Collins and B. Waldman, *Phys. Rev.* 57, 1083 (**1940**).
3. S. S. Wong, Introduction of Nuclear Physics, Wiley-VCH (**1999**), p. 105.
4. E. M. Lyman, A. O. Hanson, and M. B. Scott, *Phys. Rev.* 84, 626 (**1951**).
5. H. F. Ehrrenberg, R. Hofstadter, U. Meyer-Berkhout, D. G. Ravenhall, and S. E. Sobottka, *Phys. Rev.* 113, 666 (**1959**).
6. T. D. Forest, Jr. and J. D. Walecka, *Advan. Phys.* 15, 1 (**1966**).
7. G. Bertsch, J. Borysowicz, H. McManus, and W. G. Love, *Nucl. Phys.* A284, 399 (**1977**).
8. B. A. Brown and B. H. Wildenthal, *Annu. Rev. Nucl. Part. Sci.* 38, 29 (**1988**).
9. A. Yokoyama, *J. Phys.: Conf. Ser.* 20, 143 (**2005**).
10. K. S. Jassim, *Chinese Journal of Physics* 51, 441 (**2013**).
11. K. S. Jassim and H. A. Kassim, *Rom. Journ. Phys.* 58, 320 (**2013**).
12. K. S. J. A. Z. M. Abdul-Hamza, *Armenian Journal of Physics* 7, 4 (**2014**).
13. K. S. Jassim, A. A. Al-Sammarrae, F. I. Sharrad, and H. Abu Kassim, *Phys. Rev. C* 89, 014304 (**2014**).
14. K. S. Jassim, *Chinese Journal of Physics* 51, 441 (**2013**).
15. F. A. Majeed and L. A. Najim, *Indian Journal of Phys.* 89, 611 (**2015**).
16. J. M. Yao, et al., *Phys. ReV. C* 91, 024301 (**2015**).
17. R. A. Radhi and A. Bouchebak, *Nucl. Phys. A* 716, 87 (**2003**).
18. P. J. Brussaard and W. M. Glaudemans, Shell-Model Application, North-Holland, Amsterdam (**1977**).
19. T. D. Donnelly and I. Sick, *Rev-Mod. Phys.* 56, 461 (**1984**).
20. H. Nakada, *Phys. Rev. C* 68, 014316 (**2003**).
21. B. A. Brown, B. H. Wildentha, C. F. Williamson, F. N. Rad, S. Kowalski, H. Crannell, and J. T. O'Brien, *Phys. Rev.* C32, 1127 (**1985**).
22. B. A. Brown, R. Radhi, and B. H. Wildenthal, *Phys. Rev.* 101, 313 (**1983**).
23. P. M. End and At, *Data Nucl. Nuclear Data Tables* 23, 3AT (**1979**).
24. K. Dybal, J. S. Forster, P. Hornshj, N. Rud, and C. A. Straede, *Nucl. Phy. A* 359, 431 (**1981**).
25. G. C. Li, M. R. Yearian, and I. Sick, *Phys. Rev. C* 9, 1861 (**1974**).
26. U. P. E. A. Berg, *Phys. Lett. B* 140, 191 (**1984**).
27. H. Zarek, et al., *Phys. Lett.* 80B, 2 (**1978**).
28. Y. Horikawa, Y. Tovizuka, and A. Nakada, *Phys. Lett.* 39B, 9 (**1971**).

ARTICLE